Distributed vibration sensor based on space-division multiplexed reflectometer and interferometer in multicore fiber

Zhiyong Zhao, Ming Tang, *Senior Member, IEEE,* Liang Wang, *Member, IEEE,* Nan Guo, Hwa Yaw Tam, *Fellow, OSA,* and Chao Lu, *Fellow, OSA*

Abstract—The maximum detectable vibration frequency by phase-sensitive optical time-domain reflectometer (Φ-OTDR) is limited by the repetition rate of the pump pulse. Additionally, the intensity-demodulation based Φ-OTDR sensor suffers from the generally nonlinear dependency of the backscattered optical intensity on vibration. This makes quantitative measurement of vibration frequency difficult. In order to mitigate these limitations, we propose and demonstrate a multicore fiber (MCF) based space-division multiplexed (SDM) Φ-OTDR and Mach-Zehnder interferometer (MZI) hybrid sensor, enabling truly uninterrupted distributed vibration sensing with broad vibration frequency response range and high spatial resolution. By taking advantage of highly integrated multiple spatial cores offered by a MCF, Φ-OTDR implemented in one of the cores is used to locate the vibration. Meanwhile, a MZI is constructed using another two parallel spatial cores with sufficient continuous-wave (CW) optical power from a coherent narrow linewidth laser, which is used to retrieve the vibration frequency by processing the acquired interference signal. Compared with the single mode fiber based hybrid systems, the proposed SDM configuration allows implementation of Φ-OTDR and MZI independently without any crosstalk between them. Consequently it offers many unique advantages, such as simple data processing procedure, good signal-to-noise ratio (SNR) of the demodulated vibration frequency spectrum, no frequency dead zone, and single-end access. This cost-effective SDM hybrid sensor provides significant potential for distributed and accurate monitoring of vibrations.

Z. Zhao, N. Guo, and C. Lu are with the Photonics Research Centre, Department of Electronic and Information Engineering, The Hong Kong Polytechnic University, Hong Kong (e-mail: zhiyong.zhao@polyu.edu.hk; neil.nan.guo@outlook.com; chao.lu@polyu.edu.hk).

M. Tang is with the National Engineering Laboratory of Next Generation Internet Access Networks, School of Optical and Electronic Information, Huazhong University of Science and Technology, Wuhan 430074, China (e-mail: tangming@mail.hust.edu.cn).

L. Wang is with the Department of Electrical Engineering, The Chinese University of Hong Kong, Hong Kong (e-mail: lwang@ee.cuhk.edu.hk).

H.-Y. Tam is with the Department of Electrical Engineering, The Hong Kong Polytechnic University, Kowloon, Hong Kong (e-mail: hwa-yaw.tam@polyu.edu.hk).

Index Terms—Multicore fiber, space-division multiplexing, distributed optical fiber sensor, vibration sensing.

I. INTRODUCTION

Distributed fiber optic vibration sensor is a useful tool to evaluate the health condition of structures through analyzing the measured characteristic frequency of vibrations. It is useful to predict the potential structural defect, like the crack of concrete, deformation of rail, etc. The technology has attracted considerable interest over the last decade due to its effective non-destructive testing ability [1]. On the other hand, distributed fiber optic vibration sensing has also been intensively investigated for intrusion detection [2], where its capability of long-range sensing is important for pipeline monitoring in oil and gas industry, perimeter security, etc. Phase-sensitive optical time-domain reflectometer (Φ-OTDR) is one of the most promising solutions for distributed vibration sensing [3]. However, the maximum detectable vibration frequency of Φ-OTDR is ultimately limited by the repetition rate of the pump pulse, which becomes an intrinsic shortcoming of this technology. What's more, it should be pointed out that the most widely used direct detection intensity-demodulation (DDID) based Φ-OTDR sensor suffers from the nonlinear dependency of the backscattered optical intensity on vibration, except for very small perturbation, or it may show random intensity variation [3-5]. Therefore, sometimes quantitative vibration frequency measurement might be difficult to be achieved. Although phase- instead of intensity-demodulation has been proposed to obtain vibration frequency based on the linear relationship between the phase and the external vibration, it is at the expense of system complexity [6]. Additionally, phase noise becomes a severe problem that degrades the performance of the system [3, 7].

In order to address the limitations of intensity-demodulation based Φ-OTDR sensors, a hybrid Φ-OTDR and Mach-Zehnder interferometer (MZI) sensor using single mode fiber (SMF) has been proposed [8], which is able to simultaneously locate the external disturbance point and measure its vibration frequency. Unfortunately, the backscattered light from the offset CW light has led to significant degradation of the system SNR, and the weak optical power of the interference signal results in noisy signal power spectrum. Moreover, superposition of the pulse on the MZI interference spectrum also increases the complexity of data processing. A time-division multiplexed hybrid system is then proposed [9]. But

the measurement of MZI and Φ-OTDR is temporally separated, so the whole sensing process is essentially discontinuous, which restricts the frequency measurement range of the system. Frequency-division multiplexed hybrid system has also been demonstrated [10], but a reference fiber that has similar length to that of the sensing fiber is required to construct the MZI configuration, which will however reduce the reliability of the system since the very long reference fiber is also very sensitive to external environment, including temperature change and vibration. Additionally, it must be pointed out that another common drawback of those reported schemes is that the effective sensing length is half of the total fiber length due to the fold-back configuration.

Recently, space-division multiplexed (SDM) distributed fiber sensors using multicore fiber (MCF) have been developed, showing great potential to enable performance enhancement, e.g. achieving shape sensing [11], elimination of the cross sensitivity of temperature and strain [12, 13], large dynamic range and high measurement resolution [14]. In this paper, we propose and demonstrate experimentally a MCF based space-division multiplexed hybrid Φ-OTDR and MZI sensor without the drawbacks mentioned above. Specifically, the MZI is constructed by using two parallel spatial cores of the MCF, and its output is delivered to the transmitter side through the third spatial core, enabling single-end access. The MZI is used to retrieve vibration frequency by processing the interference spectrum with Fast Fourier Transform (FFT). Meanwhile, Φ-OTDR is implemented using the fourth spatial core to locate the vibration. In this way, both MZI and Φ-OTDR are spatially separated but implemented in the same MCF using space-division multiplexing, thus it effectively eliminates the constraint of the hybrid system implemented in SMF. In addition, since both cores of the MZI are within the same MCF, any environment variation (e.g. temperature variation) induced difference on the cores is minimized. The proposed system enables truly uninterrupted distributed vibration sensing with broadband vibration frequency response (up to 12 kHz which is limited by the cut-off frequency of the voltage driver of the transducer) and high spatial resolution (1 m over 2.42 km sensing range). Compared with hybrid sensing system using SMF, the proposed SDM hybrid sensing system using MCF enables simpler data processing procedure, much higher SNR of the power spectrum, no frequency dead zone, single-end access, etc. Therefore, it shows great potential for structural health monitoring, intrusion detection, and many other applications.

II. Measurement Principle

In the proposed MCF based space-division multiplexed hybrid Φ-OTDR and MZI sensor, the Φ-OTDR is used to locate the disturbance positions, which requires a narrow linewidth coherent laser in the system. The Rayleigh backscattered light from a pump pulse of duration W will interfere coherently at the receiver, yielding speckle-like time-domain signal trace, whose intensity is governed by [14, 15]

$$P(t) = \sum_{m=1}^{N} a_m^2 \exp\left(-2\alpha \frac{c\tau_m}{n_f}\right) rect\left(\frac{t-\tau_m}{W}\right) + \\ 2\sum_{m=1}^{N}\sum_{n=m+1}^{N} a_m a_n \cos\phi_{mn} \exp\left\{-\alpha \frac{c(\tau_m+\tau_n)}{n_f}\right\} rect\left(\frac{t-\tau_m}{W}\right) rect\left(\frac{t-\tau_n}{W}\right)$$

(1)

where N is the total number of scattering points; a_m and a_n are the amplitudes of the scattered waves; α and n_f are attenuation coefficient and refractive index of the fiber respectively; c is velocity of light in vacuum; τ_m is round trip time from input to the i-th scattering point at z_m with $\tau_m = 2n_f z_m / c$; $\phi_{m,n}$ represents the phase difference between the m-th, and the n-th scattering points with $\phi_{m,n} = 4\pi n_f \nu(z_m - z_n)/c$, in which ν is the laser frequency. In a disturbed situation, external vibration modifies the local refractive index of the sensing fiber and thus varies the phase difference $\phi_{m,n}$, which will alter the measured Rayleigh backscattered optical intensity at the perturbation point. Therefore, by subtracting a Φ-OTDR trace from a reference trace, the perturbation position is determined by the location where optical intensity variation occurs.

However, the maximum detectable vibration frequency by Φ-OTDR is limited by the repetition rate of the pump pulse, and in the DDID based Φ-OTDR sensor, the backscattered optical intensity variation is generally nonlinear to external vibration, except for very small perturbation. In the proposed SDM reflectometer and interferometer hybrid sensor, the measurement of vibration frequency can be carried out by the MZI instead of the Φ-OTDR, while Φ-OTDR is only used to locate the positions of vibrations. Thanks to the distinctive structure of multiple parallel spatial cores of the MCF, a unique MZI can be constructed using two independent cores of the MCF as its two arms. Assume the output electric fields of the light from two arms of the MZI are given by $E_1(t)e^{j[\omega t+\varphi_1(t)]}$ and $E_2(t)e^{j[\omega t+\varphi_2(t)]}$, respectively. Then the output intensity $I(t)$ of the interferometer can be expressed by

$$I(t) \propto E_1^2(t) + E_2^2(t) + 2E_1(t)E_2(t)\cos(\theta_P)\cos[\varphi_1(t) - \varphi_2(t)]$$

(2)

where ω is the optical angular frequency, $\varphi_1(t)$ and $\varphi_2(t)$ are optical phases of the light, θ_P is the relative polarization angle of the light between the two arms.

It has been reported that the cores of MCF will undergo local tangential strain when the MCF is curved [11, 16-17], as shown in Fig. 1. For a specific bending radius, the strain is essentially dependent on the angular position of the core, as given by [11]

$$\varepsilon_i = -\frac{d_i}{R}\cos(\theta_b - \theta_i)$$

(3)

Where ε_i is the bending induced strain in core i, d_i is the distance between core i and the fiber center, R is the bending radius, θ_b and θ_i are respectively the bending angle and the angular position of core i.

Vibrations applied to the sensing fiber will alter the curvature of the sensing fiber; as a result the cores will experience different strain variation and consequently different phase change. Due to the vibration induced change of light phase difference between the two MZI arms, as well as the modification of relative polarization angle, the output optical intensity of the interferometer will vary accordingly. In this way, the vibration frequency can be obtained by processing the sampled interference spectrum with FFT. It should be pointed out that due to the all-solid compact and uniform arrangement of spatial cores in the single MCF along the whole fiber range, the MZI in the proposed SDM hybrid sensor has much better tolerance against external noise. Any common environment variation (e.g. temperature variation) will cause the same phase change in the two spatial cores, and will not affect the interferometer output. Therefore the reliability of the hybrid system is enhanced significantly. Another advantage of the proposed SDM configuration is that the output signal of the MZI can be transmitted back to the transmitter side through the third spatial core and then detected, which is very useful in practical fiber deployment with the single-end access ability.
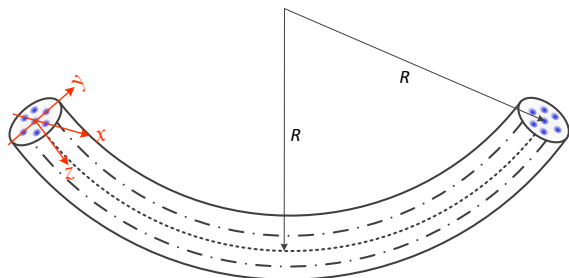

Fig. 1. Schematic diagram of the bent MCF with a bending radius of R. bending will generate different local tangential strains in distinct spatial cores.

III. EXPERIMENTAL SETUP

The experimental setup used for the proposed SDM Φ-OTDR and MZI hybrid sensing system is shown in Fig. 2. A coherent laser source with ~10 kHz linewidth has been used in the experiment, whose coherence length is about 6.4 km. The CW output of laser is divided into two branches through a 50:50 coupler. The upper branch is then further split into two paths and light in the two paths are then launched into core 1 and core 2 respectively through a fan-in coupler. Core 1 and core 2 form the two arms of the MZI. A tunable attenuator is inserted to manage the input power flexibly. The fiber under test (FUT) is a seven core fiber with 2.42 km length. At the far end, the output of the two cores from the fan-out coupler is combined again by a coupler to construct the MZI, and the coupler output is then connected to core 4, by which the interference signal of the MZI is transmitted back to the transmitter side, and is eventually detected by a 125 MHz photodetector (PD1). In this way, a MZI enabling single-end access is achieved, and sufficient optical power is available to ensure high SNR for the interference spectrum. On the other hand, the lower branch is used to implement Φ-OTDR. An electro-optic modulator (EOM) driven by an electrical pulse

generator with 10 ns duration is used to generate the pump pulse. The pulse is then amplified by an erbium-doped fiber amplifier (EDFA), and passes through an optical band-pass filter to minimize the amplified spontaneous emission (ASE) noise. The power boosted pulse is then launched into core 3 through a circulator and the fan-in coupler. At the receiver side of the reflectometer, the backscattered Rayleigh signal is detected by a 200 MHz photodetector. The two detectors are connected to an oscilloscope for data acquisition, which is controlled by a computer with LabVIEW program.
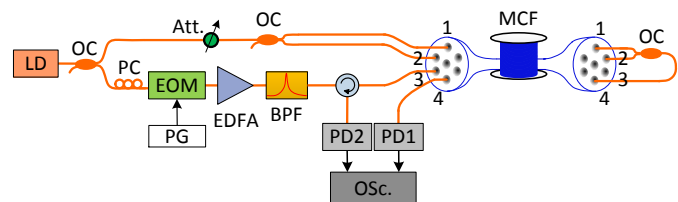

Fig. 2. Experimental setup for the SDM reflectometer and interferometer hybrid sensor. LD: Laser diode; OC: optical coupler; PC: polarization controller; Att.: tunable attenuator; EOM: electro-optic modulator; PG: pulse generator; EDFA: erbium-doped fiber amplifier; BPF: band-pass filter; PD: photodetector; OSc.: oscilloscope.

The cross sectional view of the MCF (YOFC, China) used in the experiment is shown in Fig. 3(a), which has 150 μm cladding diameter and 42 μm core-core pitch with the outer six cores arranged hexagonally. In order to suppress crosstalk, the cores have been designed to be surrounded by deep trench. The packaged fan-in/out coupler is shown in Fig. 3(b), which contains seven SMF pigtails and a MCF pigtail; it ensures independent coupling of each core of the MCF to the corresponding SMF pigtail. The configuration of the FUT is shown in Fig. 3(c), which consists of five sections. In order to generate controllable vibrations, two short fiber sections (1.6m and 1.9m long) have been wound on two piezoelectric transducers (PZTs), respectively. The PZTs are driven by a high voltage driver, and an arbitrary waveform generator (AWG) is used to apply periodic sinusoidal signals. It should be pointed out that the electrical cut-off frequency of the high voltage driver is less than 13 kHz, which determines the available maximum vibration frequency in our lab.
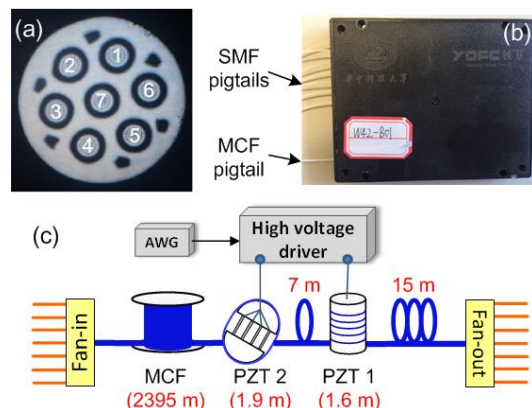

Fig. 3. (a) Cross section of the seven-core MCF; (b) the packaged MCF fan-in/out coupler; (c) configuration of the FUT for vibration sensing; AWG: arbitrary waveform generator. PZT: piezoelectric transducer.

In the proposed SDM reflectometer and interferometer hybrid sensor, the Φ-OTDR and MZI share the same laser source, but are implemented in different spatial cores, which ensures that both interrogations are conducted simultaneously and independently. Therefore, the constraint of the hybrid system using SMF can be completely eliminated. On one hand, continuous acquisition with sufficient optical power but without superposition of pulse response is ensured for the interferometer. On the other hand, high SNR can be achieved for the measurements of both Φ-OTDR and MZI. The data processing procedure can also be simplified, since there is no need to separate the acquired data between the two.

IV. RESULTS AND DISCUSSION

A. Detection of single vibration event

Based on the proposed SDM hybrid reflectometer and interferometer sensor, experiment has been carried out by applying 5 kHz vibration on PZT 1 to detect the single vibration event. Fig. 4(a) shows the measured Φ-OTDR trace along the sensing fiber, which has been averaged by 256 times in order to increase the SNR. 10 ns pump pulse was used with corresponding spatial resolution of 1m. To locate the vibration, consecutive traces are measured and then subtracted from an undisturbed reference trace. The superimposed differential Φ-OTDR traces are presented in Fig. 4(b). The inset in Fig. 4(b) shows the zoom-in view around the vibration point. It indicates that the vibration event can be successfully monitored and located with high SNR. It is found that intensity change occurs at about 3 m region in the differential Φ-OTDR traces. Note that 1.6 m long sensing fiber is wound to PZT 1, so the result is reasonable considering the 1 m spatial resolution.
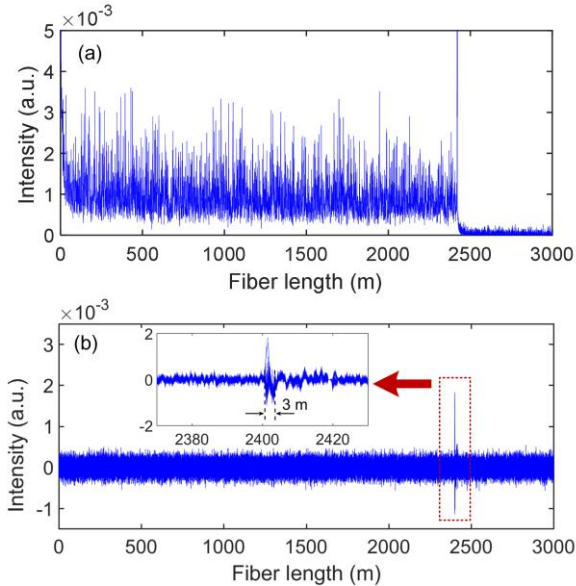

Fig. 4. (a) The measured Φ-OTDR trace along the MCF; (b) 100 consecutive differential Φ-OTDR traces superimposed together. The inset shows the enlarged view around the vibration point introduced by PZT 1.

On the other hand, the measurement of the interferometer has also been conducted simultaneously. Fig. 5(a) shows the

measured time-domain interference signal within 10 seconds duration when 5 kHz sinusoidal signal is applied to PZT 1. In order to see clearly the characteristics of the interference signal, Fig. 5(b) presents a zoom-in view of the interference signal, which indicates that high fringe contrast is achieved. The acquired time-domain interference signal is then transformed to frequency domain by FFT, and the retrieved frequency spectrum is presented in Fig. 5(c). The inset in Fig. 5(c) presents the retrieved frequency spectrum with the vertical axis showing in linear coordinate. The dominate peak is found to appear at 5 kHz, which matches very well with the applied value. Thanks to the sufficient optical power at the receiver and high fringe contrast of the interference signal, about 38 dB SNR is achieved for the measurement. In addition, high order harmonics have also been observed in the retrieved frequency spectrum, the second and the third harmonics are respectively 8.52 dB and 13.79 dB lower than the fundamental frequency. As can be seen from the inset of Fig. 5(c), also has been verified by many other measurements, the amplitudes of the high order harmonics are actually much lower than the fundamental frequency so that they are negligible in the linear coordinate, and this won't affect the correct determination of the real vibration frequency.
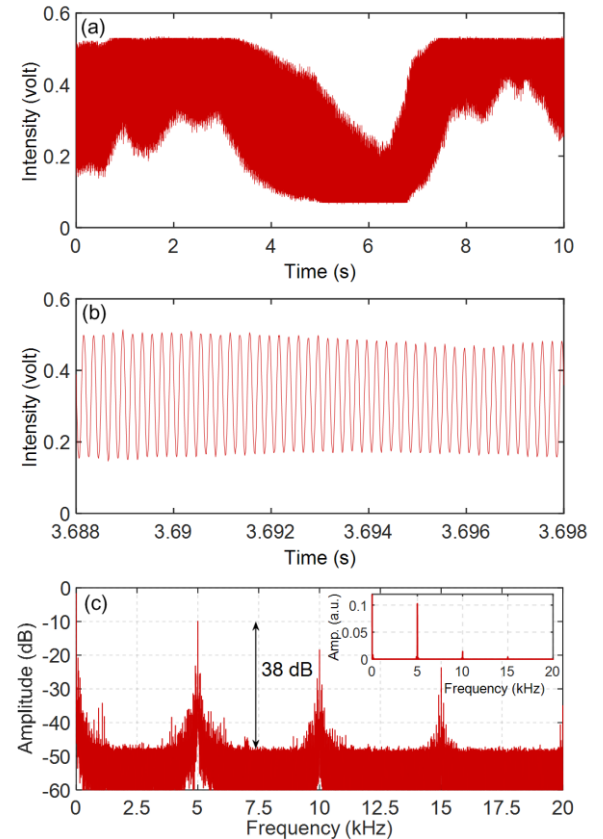

Fig. 5. (a) The measured time-domain interference signal of MZI within 10 seconds when the vibration with 5 kHz frequency is introduced by PZT 1; (b) zoom-in view of the interference signal; (c) the retrieved frequency spectrum after FFT of the signal in (a); the inset presents the frequency spectrum with the vertical axis showing in linear coordinate.

In the intensity-demodulation based MZI, the output power is governed by equation 2, which is a function of the phase

difference between its two arms. Essentially, the high order harmonics in the retrieved frequency spectrum in Fig. 5(c) are generated due to the reason that vibration induced phase change is not within a monotonic interval (i.e. either the rising interval or the falling interval) of the cosine transmission spectrum of the MZI, as schematically shown in Fig. 6(a). In this case, the variation of output optical power will not vary conformably as the trend (frequency) of vibration, but subjects to a modulation by the cosine function. As a result, high order harmonics will come into being in the frequency spectrum that is retrieved by FFT.
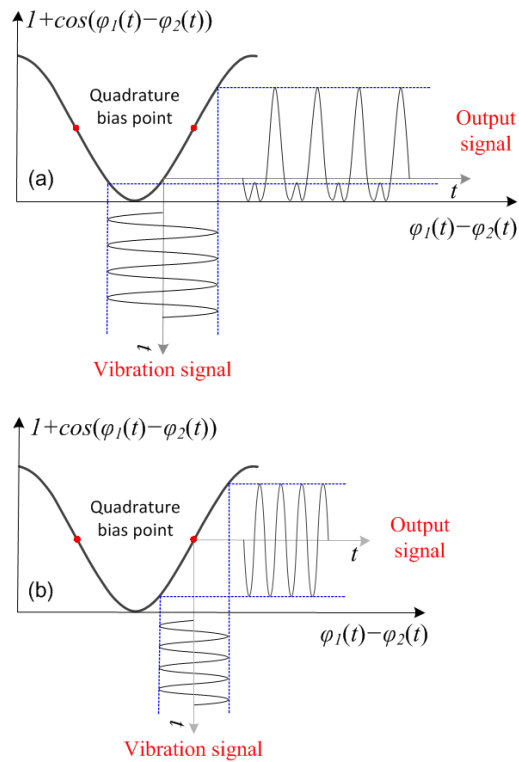

Fig. 6. Schematic diagram of the response of system on vibration when perturbation induced phase change is (a) not within and (b) within a monotonic interval of the cosine transmission spectrum of the MZI.

It turns out that absolute consistency of variation between the vibration signal and the output optical power of MZI can be ensured if perturbation induced phase change is within a monotonic interval of the cosine transmission spectrum of the MZI. Then an effective way to maintain the consistency is to make the initial bias point of the MZI working at the quadrature point, as has been marked in Fig. 6(b). This can be done by inserting a tunable delay line into one of the two arms of the MZI, and by adjusting the phase difference between the two arms to make sure that the working point of MZI is set at the quadrature point. In this way, the variation of output power of MZI will be completely consistent with the trend (frequency) of vibration signal. In addition, another benefit of this setting is that high sensitivity can be achieved when working at the quadrature point of the cosine transmission curve.

The best advantage of the intensity-demodulation based MZI setup is the simplicity in both the system configuration and the demodulation algorithm. While it should be mentioned

that phase instead of intensity detection is a better solution in order to achieve good linearity between the vibration signal and the output optical signal, so that the high order harmonics in frequency spectrum can be avoided. In addition to the traditional coherent detection method, phase generated carrier (PGC) technique has been used in both Φ-OTDR and the interferometric sensors [18-21], which shows good feasibility to acquire the phase information of the MZI in this system. But of course this is achieved at the expense of increasing system complexity.
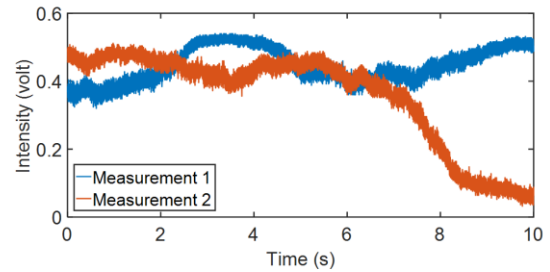

Fig. 7. The measured output interference signal of the MZI when there is no vibration applied to the sensing fiber.

It is found that there is a slow envelope change in the interference spectrum in Fig. 5(a), which is caused by phase noise that comes from the indoor air flow induced shaking on the short free MCF section, as well as the wavelength drift of the laser. In order to verify this, the output signal of the MZI without vibration applied on the sensing fiber has also been record for comparison, as shown in Fig. 7. Two separate measurements have been implemented, which reveals that the output is not constant but shows intensity fluctuation resulting from the phase noise. However, it is found that the phase noise has the feature of low frequency and weak power spectrum amplitude, as can also be seen from Fig. 5(c). So it won't lead to severely detrimental impact on the measurement. The frequency components around the vibration frequency in Fig. 5 (c) are the beat interference that is caused by the beating between the external interferences (including ambient noise, laser frequency instability and electrical noise) induced low frequency signals and the vibration signal. Fortunately, the amplitudes of beat interferences are much smaller than that of the peak frequency of the signal to be detected, so it will not affect the result of measurement.
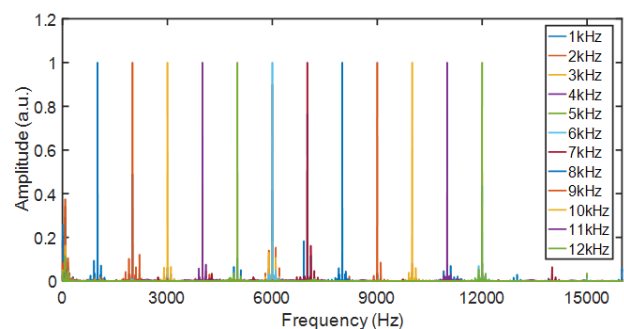

Fig. 8. FFT spectra of the interference signal measured by the MZI when the vibration by PZT 1 is applied to the sensing fiber with vibration frequency from 1 kHz to 12 kHz at 1 kHz interval.

In order to evaluate the reliability of the SDM hybrid sensor, repeated vibration measurements have been performed by applying different vibration frequencies to PZT 1, i.e. from 1 kHz to 12 kHz (maximum achievable frequency in our lab) at 1 kHz interval. For all the vibration frequencies, Φ-OTDR exactly locates the vibration by PZT 1. Meanwhile the output interference signal of the MZI is recorded, and then used for calculating the FFT frequency spectrum. The retrieved normalized frequency spectra have been shown in Fig. 8. The result confirms the excellent reliability of the hybrid sensor for vibration sensing. Additionally, it also verifies a distinguished SNR of the FFT spectra. Since the noise level is very low in Fig. 8, which ensures sufficient SNR budget to achieve vibration measurement of higher vibration frequency beyond the one presented in this work.

B. Detection of multiple simultaneous vibration events

In the previous section, experiments have demonstrated the detection of single vibration event and successfully retrieved the vibration location and frequency based on the proposed SDM Φ-OTDR and MZI hybrid sensing system. However, in practical applications, multiple vibration events may occur simultaneously. Therefore experiment has also been carried out to investigate the feasibility of simultaneous multi-event sensing based on the proposed hybrid sensor.
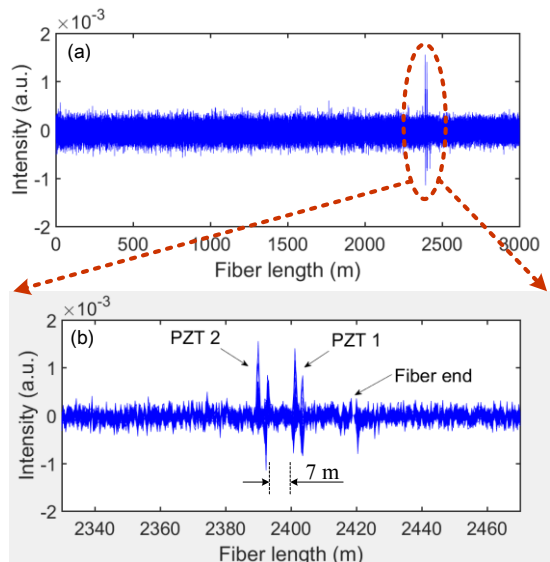

Fig. 9. (a) The superimposed 100 consecutive differential Φ-OTDR traces when simultaneous vibrations are applied by PZT 1 and PZT 2 with frequencies of 500 Hz and 300 Hz, respectively; (b) the enlarged view around the vibration locations.

For proof of concept, two vibrations with frequencies of 500 Hz and 300 Hz have been simultaneously applied by PZT 1 and PZT 2, respectively. Continuous acquisition of the time-domain traces of Φ-OTDR is performed, and the differential traces are obtained by subtracting them from a reference trace. Fig. 9(a) shows 100 consecutive differential Φ-OTDR traces superimposed together, where vibration signals can be identified with sufficient SNR at the far end. In order to see clearly the disturbed region, a zoom-in view around the

vibration points has been presented in Fig. 9(b), where two vibrations with a distance of 7 m between them can be clearly observed. The result matches very well with the spatial arrangement of FUT (see Fig. 3(c)), thus verifies the capability and reliability of locating multiple vibrations by the Φ-OTDR of the SDM hybrid sensor.
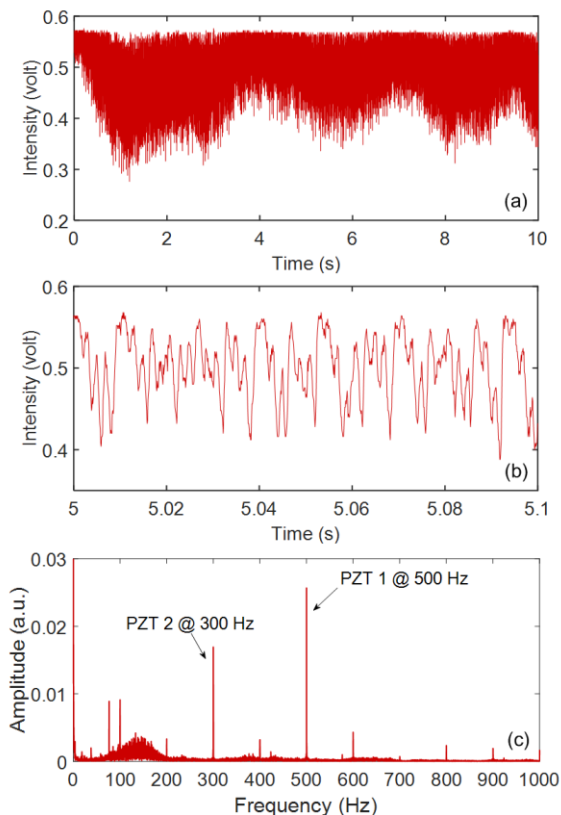

Fig. 10. (a) The measured time-domain interference signal of MZI within 10 seconds when two vibrations are applied by PZT 1 and PZT 2 with 500 Hz and 300 Hz frequencies, respectively; (b) zoom-in view of the interference signal; (c) the retrieved frequency spectrum after FFT of the signal in (a).

Meanwhile, in parallel with the detection of the vibration location by Φ-OTDR, the measurement of the vibration frequency by the MZI of the SDM hybrid sensor has also been carried out. Fig. 10(a) shows the measured interference signal of the MZI within 10 seconds. Fig. 10(b) presents a zoom-in view of Fig. 10(a) for better observation. By implementing FFT on the sampled interference signal, the retrieved frequency spectrum is presented in Fig. 10(c). Two dominant peaks are observed at 500 Hz and 300 Hz, respectively, which is consistent with the applied frequencies, as marked in the figure. So it demonstrates that the locations of multiple simultaneous vibration events can be determined with the help of Φ-OTDR, and their vibration frequencies can be retrieved through the measurement of MZI. Further, in order to determine the vibration frequency of each identified vibration location, frequency mapping method can be employed [10], if the frequencies of multiple vibrations are not exactly the same. The method requires that both MZI and Φ-OTDR are used to measure the vibration frequencies, and the measurement of Φ-OTDR is implemented with under-sampling. Then frequency

mapping is achieved through comparing the frequencies that are measured by Φ-OTDR and MZI with a specific mathematical relation, as given by

$$f_{\phi-OTDR} = \left| f_{MZI} - k \cdot f_s \right| \quad \left(\left| f_{MZI} - k \cdot f_s \right| < f_s / 2 \right) \quad (4)$$

Where $f_{\phi-OTDR}$ and f_{MZI} are the frequencies that are measured by Φ-OTDR and MZI, respectively; k is an integer and f_s is the sampling frequency of Φ-OTDR. Once two specific frequencies from the measurements of Φ-OTDR and MZI match well with equation 4, then the frequency mapping is successful. In this way, each frequency that is retrieved through MZI can be targeted to a specific vibration location that is identified by Φ-OTDR.

As a matter of fact, in addition to the distributed sensing method based on OTDR technique, long range optical fiber interferometers have also been used for distributed vibration sensing, which normally adopt the system configurations of two interferometers, including Mach-Zehnder interferometer, Sagnac interferometer and Michelson interferometer, and event positioning is achieved generally based on the time delay estimation algorithm [23-25]. Thanks to the unique structure of multiple cores embedded in the MCF, it provides an excellent platform to implement the long range interferometers, which indeed provides a potential way to achieve distributed multi-point vibration sensing [23].
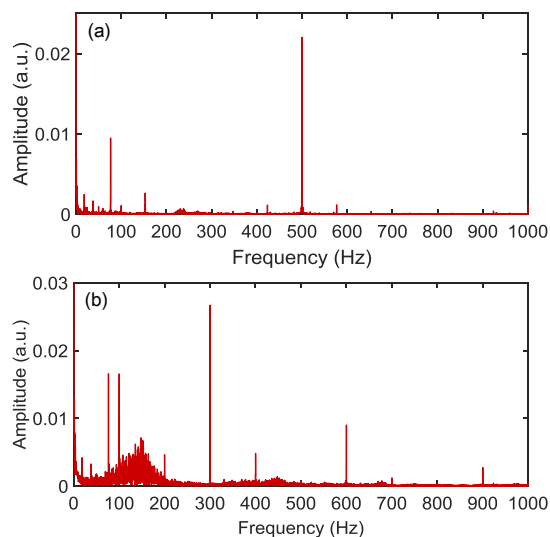

Fig. 11. The retrieved frequency spectra when single vibration is applied by (a) PZT 1 with 500Hz frequency; (b) PZT 2 with 300Hz frequency.

In Fig. 10(c), in addition to the two dominant peaks, some minor harmonic components are also observed. Particularly it is found that there is a noise band approximately located between 80 Hz to 200 Hz. The noise band is found to be caused by PZT 2, due to the fact that PZT 2 is actually a fiber stretcher that consists of four parallel piezo stacks (see the picture in Ref. [22]). The slight difference of stack lengths and piezoelectric coefficients lead to the detuned oscillation noise, yielding impure vibrations. For comparison, Fig. 11(a) and

11(b) present the obtained FFT spectra when single vibration is applied by PZT 1 with 500 Hz frequency, and PZT 2 with 300 Hz frequency, respectively. It is found that the noise band still exists in the frequency spectrum of the vibration generated by PZT 2 but disappear in the one generated by PZT 1. Additionally, the small peak at 80 Hz in the figures is believed to be caused by the electrical noise of the high voltage driver, since it appears in all the measurements.

C. Discussion

It should be pointed out that if the vibration amplitude is small enough, it is possible to measure it quantitatively, because the bending induced phase change is a function of the bending radius of the fiber, as inferred from equation 3. In addition, the measurement sensitivity of MZI is dependent on its working bias point.

Compared with the hybrid sensing systems using SMF, the proposed SDM hybrid sensor based on MCF ensures sufficient optical power injected into the sensing fiber for the MZI, thus much better SNR can be obtained and consequently high measurement accuracy of the vibration frequency is ensured. On the other hand, the Φ-OTDR in the proposed hybrid system is only used for locating the vibration. So it does not require fast data acquisition, and hence trace averaging can be employed, which will help to increase the SNR of measurement and eventually ensure high positioning accuracy and high spatial resolution. Due to the separate implementation of the Φ-OTDR and MZI using space division multiplexing, the data measured by the reflectometer and interferometer are independently collected, which gives rise to much simpler data processing procedure. More importantly, the proposed hybrid sensor manages to get rid of the detrimental impact of CW light on Φ-OTDR which exists in the hybrid system using SMF. The MCF provides redundant core for transmitting the output of the interferometer back to the transmitter side, enabling singe-end access. In the time-division multiplexed hybrid system, the minimal detectable frequency is determined by the repetition rate of pulse, so there will be a frequency dead zone [9]. However, in the proposed hybrid system, the detection and acquisition of MZI are continuous, so it has no dead zone. Note that the maximum detectable vibration frequency of the proposed system is essentially determined by the sampling frequency of the oscilloscope and the bandwidth of the photodetector, so apparently it would achieve very broadband frequency response without any dead zone in the detectable range.

At last, it should be pointed out that it is difficult to achieve comparable performance by using SMFs bundle instead of the MCF in the proposed system deployment. This is because the MCF integrates all-solid cores together, and thus the physical path of each core is strictly identical along the whole fiber length. This highly integrated fiber structure enables the system to eliminate the common environment noise (e.g. temperature variation), but output the differential response (e.g. vibration induced differential strain). While the bundle of SMFs cannot be as compact and uniform as the MCF, especially along very long range. In this case, it is difficult to ensure that the external environment variation has identical

impact on the two arms of the MZI, especially for the case where multiple SMFs are bundled loosely, which will lead to strong noise. For the hybrid system using a bundle of SMFs, nonlinear relative phase change between the two arms might be introduced because of the distinct amounts of transformation from external disturbance (e.g. temperature and strain). All these factors will eventually degrade the accuracy and reliability of the SMFs bundle based hybrid system. In addition, it is worth mentioning that considering the cost of optical fiber cable instead of the fiber itself, seven-core fiber cable is actually cheaper than the seven separate SMF cables, which makes our hybrid system based on MCF more cost-effective.

V. CONCLUSION

In conclusion, we have proposed and experimentally demonstrated a multicore fiber based space-division multiplexed Φ-OTDR and MZI hybrid sensing system. Taking advantage of the multiple spatial cores offered by the MCF, the reflectometer and interferometer manage to be implemented in separate cores with a shared narrow linewidth laser source, thus independent interrogation of each sensor has been achieved. This completely eliminates the constraint of hybrid systems using SMF. The proposed SDM hybrid sensor is able to locate the vibration point and measure the vibration frequency simultaneously with high reliability, and enables truly uninterrupted distributed vibration sensing with broad vibration frequency response range and high spatial resolution. Specifically, 2.42 km sensing range with 1 m spatial resolution and up to 12 kHz vibration sensing have been demonstrated in the experiment. In addition, multiple simultaneous vibration events can be located with the help of Φ-OTDR, and their vibration frequencies are retrieved through the measurement of MZI. Compared with hybrid systems using SMF, the SDM solution using MCF shows many unique advantages, e.g. much higher SNR of measurements, higher measurement accuracy, higher tolerance against external noise, simpler data processing procedure, no frequency dead zone, single-end access, robust and high reliability, etc. Therefore, it is believed that the SDM Φ-OTDR and MZI hybrid sensor will have great potential for long-haul distributed vibration sensing applications.

ACKNOWLEDGMENT

REFERENCES

[1] X. Bao, D. Zhou, C. Baker, and L. Chen, "Recent development in the distributed fiber optic acoustic and ultrasonic detection," *J. Lightw. Technol.,* vol. 35, no. 16, pp. 3256–3267, Aug. 2017.

[2] F. Peng, H. Wu, X. Jia, Y. Rao, Z. Wang, and Z. Peng, "Ultra-long high-sensitivity Φ-OTDR for high spatial resolution intrusion detection of pipelines," *Opt. Exp.,* vol. 22, no. 11, pp. 13804–13810, 2014.

[3] X. Fan, G. Yang, S. Wang, Q. Liu, and Z. He, "Distributed fiber-optic vibration sensing based on phase extraction from optical reflectometry," *J. Lightw. Technol.,* vol. 35, no. 16, pp. 3281-3288, Aug. 2017.

[4] H. F. Martins, S. Martin-Lopez, P. Corredera, M. L. Filograno, O. Frazao, and M. Gonzalez-Herraez, "Coherent noise reduction in high visibility phase sensitive optical time domain reflectometer for distributed sensing of ultrasonic waves," *J. Lightw. Technol.,* vol. 31, no. 23, pp. 3631–3637, Dec. 2013.

[5] J. Tejedor et al., "Toward prevention of pipeline integrity threats using a smart fiber-optic surveillance system," *J. Lightw. Technol.,* vol. 34, no. 19, pp. 4445–4453, Oct. 2016

[6] Z. Wang, L. Zhang, S. Wang, N. Xue, F. Peng, M. Fan, W. Sun, X. Qian, J. Rao, and Y. Rao, "Coherent Φ-OTDR based on I/Q demodulation and homodyne detection," *Opt. Exp.,* vol. 24, no. 2, pp. 853–858, Jan. 2016.

[7] Z. Pan, K. Liang, Q. Ye, H. Cai, R. Qu, Z. Fang, "Phase-sensitive OTDR system based on digital coherent detection," *Proc. SPIE,* vol. 8311, pp. 83110S1-S6, 2011.

[8] T. Zhu, Q. He, X. H. Xiao, and X. Y. Bao, "Modulated pulses based distributed vibration sensing with high frequency response and spatial resolution," *Opt. Exp.,* vol. 21, no. 3, pp. 2953–2963, Feb. 2013.

[9] Q. He, T. Zhu, X. Xiao, B. Zhang, D. Diao, and X. Bao, "All fiber distributed vibration sensing using modulated time-difference pulse," *IEEE Photon. Technol. Lett.,* vol. 25, no. 20, pp. 1955–1957, Oct. 2013.

[10] H. He, L. Shao, B. Luo, Z. Li, X. Zou, Z. Zhang, W. Pan, and L. Yan, "Multiple vibrations measurement using phase-sensitive OTDR merged with Mach-Zehnder interferometer based on frequency division multiplexing," *Opt. Exp.,* vol. 24, no. 5, pp. 4842-4855, Mar. 2016.

[11] Z. Zhao, M. A. Soto, M. Tang, and L. Thévenaz, "Distributed shape sensing using Brillouin scattering in multi-core fibers," *Opt. Exp.,* vol. 24, no. 22, pp. 25211–25223, Oct. 2016.

[12] Z. Zhao, Y. Dang, M. Tang, L. Duan, M. Wang, H. Wu, S. Fu, W. Tong, P. P. Shum, and D. Liu, "Spatial-division multiplexed hybrid Raman and Brillouin optical time-domain reflectometry based on multi-core fiber," *Opt. Exp.,* vol. 24, no. 22, pp. 25111–25118, Oct. 2016.

[13] Z. Zhao, Y. Dang, M. Tang, B. Li, L. Gan, S. Fu, H. Wei, W. Tong, P. Shum, and D. Liu, "Spatial-division multiplexed Brillouin distributed sensing based on a heterogeneous multicore fiber," *Opt. Lett.* vol. 42, no. 1, pp. 171–174, Jan. 2017.

[14] Y. Dang, Z. Zhao, M. Tang, C. Zhao, L. Gan, S. Fu, T. Liu, W. Tong, P. P. Shum, and D. Liu, "Towards large dynamic range and ultrahigh measurement resolution in distributed fiber sensing based on multicore fiber," *Opt. Exp.,* vol. 25, no. 17, pp. 20183-20193, Aug. 2017.

[15] Y. Koyamada, M. Imahama, K. Kubota, and K. Hogari, "Fiber-optic distributed strain and temperature sensing with very high measurand resolution over long range using coherent OTDR," *J. Lightw. Technol.,* vol. 27, no. 9, pp. 1142–1146, May. 2009.

[16] M. Gander et al., "Bend measurement using Bragg gratings in multicore fibre," *Electron. Lett.,* vol. 36, no. 2, p. 1–2, 2000.

[17] G. M. H. Flockhart, W. N. MacPherson, J. S. Barton, J. D. C. Jones, L. Zhang, and I. Bennion, "Two axis bend measurement with Bragg gratings in multicore optical fiber," *Opt. Lett.,* vol. 28, no. 6, pp. 387–389, Mar. 2003.

[18] G. Fang, T. Xu, S. Feng, and F. Li, "Phase-sensitive optical time domain reflectometer based on phase-generated carrier algorithm," *J. Lightw. Technol.,* vol. 33, no. 13, pp. 2811–2816, Jul. 2015.

[19] X. He, S. Xie, F. Liu, S. Cao, L. Gu, X. Zheng, M. Zhang, "Multi-event waveform-retrieved distributed optical fiber acoustic sensor using dual-pulse heterodyne phase-sensitive OTDR," *Opt. Lett.,* vol. 42, no. 3, pp. 442–445, Feb. 2017.

[20] J. He, L. Wang, F. Li, and Y. L. Liu, "An ameliorated phase generated carrier demodulation algorithm with low harmonic distortion and high stability," *J. Lightw. Technol.,* vol. 28, no. 22, pp. 3258–3265, 2010.

[21] G. Wang, T. Xu and F. Li, "PGC Demodulation Technique With High Stability and Low Harmonic Distortion," *IEEE Photon. Technol. Lett.,* vol. 24, no. 23, pp. 2093-2096, Dec.1, 2012.

[22] C. Jin, L. Wang, Y. Chen, N. Guo, W. Chung, H. Au, Z. Li, H. Y. Tam, and C. Lu, "Single-measurement digital optical frequency comb based phase-detection Brillouin optical time domain analyzer," *Opt. Exp.,* vol. 25, no. 8, pp. 9213–9224, Apr. 2017.

[23] Q. Sun, D. Liu, J. Wang, and H. Liu, "Distributed fiber-optic vibration sensor using a ring Mach–Zehnder interferometer," *Opt. Commun.,* vol. 281, no. 6, pp. 1538–1544, 2008.

[24] X. Hong, J. Wu, C. Zuo, F. Liu, H. Guo, and K. Xu, "Dual Michelson interferometers for distributed vibration detection," *Appl. Opt.,* vol. 50, pp. 4333–4338, 2011.

REPLACE THIS LINE WITH YOUR PAPER IDENTIFICATION NUMBER (DOUBLE-CLICK HERE TO EDIT) <   9

[25] S. J. Russell, K. R. C. Brady, and J. P. Dakin, "Real-time location of multiple time-varying strain disturbances, acting over a 40-km fiber section, using a novel dual-Sagnac interferometer," *J. Lightw. Technol.*, vol. 19, no. 2, pp. 205–213, Feb. 2001.